Communications

A Feasibility Study for Electrical Impedance Tomography as a Means to Monitor Tissue Electroporation for Molecular Medicine

Rafael V. Davalos*, Boris Rubinsky, and David M. Otten

***Abstract*—Molecular medicine involves the introduction of macromolecules, such as drugs or gene constructs, into specific cells of the body. Electroporation, which uses electric pulses to permeate cell membranes, is a method for achieving this. However, as with other molecular medicine procedures, it lacks a real-time mechanism to detect and control which cells have been affected. We propose and demonstrate, via computer simulation, that electrical impedance tomography has the potential for detecting and imaging electroporation of cells in tissue in real-time, thereby providing feedback for controlling electroporation.**

***Index Terms*—Electrical impedance tomography, electrochemotherapy, electroporation, medical imaging.**

I. Introduction

The goal of molecular medicine is to introduce macromolecules such as drugs and gene constructs into specific cells of the body. Some of the better-known molecular medicine techniques include viral vectors [1] and electroporation [2]. Electroporation, which is the focus of this study, is a physical method that uses electrical fields to temporarily increase the permeability of the cell membrane [3]. This permeation facilitates penetration of extracellular macromolecules that could otherwise not enter the cell [4]. For a specific set of voltage parameters (e.g., pulse number, frequency, duration), the effect that the electric field has on a cell depends on the voltage gradients that develop across the individual cell [4]. A voltage gradient, depending on its magnitude, can have one of three effects on the cell membrane: reversible permeation, in which the cell membrane reseals after the application of the pulse, irreversible permeation (i.e., cell death—in which the cell membrane does not reseal), or no change in the cell membrane. Electroporation can be used with any type of macromolecule, including drugs for cancer therapy or gene constructs for gene therapy, and is used with individual cells (*in vitro*) and with cells in the human body (*in vivo*). When electroporation is used *in vivo*, electrodes are strategically placed in the tissue and high-voltage electrical pulses are applied in such a way to produce voltage gradients that temporarily permeate the cells of a predetermined area. This facilitates the penetration of extracellular macromolecules such as drugs or gene constructs into the cells of the electroporated area [1], [5], [6]. A recent extensive book in the field of tissue electroporation is [7].

In electroporation, as in all the other molecular medicine techniques, there is currently no method to actively monitor or control the process in real-time, i.e., to determine during the procedure that indeed the cell membranes have become temporarily permeabilized in the desired area. Only the consequences of the process can be determined after the electroporation process has been completed. A procedure to ascertain whether electroporation has taken place uses fluorescent dyes and requires sacrificing the specimen [8]. However, most procedures simply observe the outcome on the cells or patient [4]. In order to reliably apply any of the molecular medicine techniques to human patients, it is necessary to actively monitor and precisely control the location at which the procedure is applied. Specifically, it is highly desirable in an electroporation procedure to know in real-time if the cells in the treated area have become electroporated or not. Such information could be used in a feedback loop to modify the electrical pulses to ensure that all of the cells in the target area will become penetrable to the treatment macromolecules, while ensuring that the other cells in the vicinity will not. Otherwise, as indicated above, only the long-term consequences of the treatment can be determined, such as the cure or lack of cure of the cancer patient or the expression or the lack of expression of a gene.

In this paper, we propose that a noninvasive imaging method known as electrical impedance tomography (EIT) [9] may be able to produce a real-time image of the area in which cells have become permeable during electroporation. EIT noninvasively produces an image of internal impedance distributions based on surface current injection patterns and measurement of the resulting surface potentials [10]. Our work is based on the hypothesis that if the cell membrane becomes permeable to macromolecules during electroporation, it should also become permeable to ions and, therefore, the electrical impedance of a cell should change measurably during electroporation. In previous experiments with a microelectromechanical chip that incorporated a live biological cell within an electric circuit, we quantified the change in conductivity of an individual cell during electroporation [11]. The results suggested that the impedance of tissue should decrease during electroporation to an extent detectable using a bioimpedance technique. This indicates that EIT could produce an image of the electroporated area. Using EIT we would be able to verify, while the patient is being treated, whether the cells in a particular area in the body have become permeabilized or not. Furthermore, EIT could be used in a feedback loop to manipulate the magnitude of the electrical pulses as well as the placement of the electrodes to induce permeabilization of the cells in a desired area.

II. Methods

In order to establish feasibility of this concept, we have developed a computer simulation of the process of electroporation in tissue and of the EIT imaging of this process. This simulation consists of a finite-element model representing the liver with a small internal section undergoing electroporation. This electroporation model is based on realistic geometric and electrical properties. The electroporated area is determined using an iterative technique with boundary conditions based on standard electrochemotherapy parameters. The data from this electroporation model is then used to generate a conductivity map for input to the EIT simulation, which then reconstructs an image of the direct model electroporated area.

The electroporation model is a simplified two-dimensional isotropic cross section of a liver 10 cm in diameter. Three electroporation electrode configurations, modeled after previous tissue electroporation experiments [12], are applied to the tissue as examples. The first configuration (Fig. 1) has four electrodes placed in a square configuration,

Manuscript received July 3, 2001; revised November 28, 2001. This work was supported by the National Institutes of Health (NIH) under Grant. 1 R21 RR15252-01. The work of R. Davalos was supported by Sandia National Laboratories. *Asterisk indicates corresponding author.*

*R. V. Davalos is with the Biomedical Engineering Laboratory, Department of Mechanical Engineering, University of California at Berkeley, 1627 University Avenue, Apt. 312, Berkeley CA 94720 USA (e-mail: rvdaval@sandia.gov).

B. Rubinsky and D. M. Otten are with the Biomedical Engineering Laboratory, Department of Mechanical Engineering, University of California at Berkeley, Berkeley CA 94720 USA.

Publisher Item Identifier S 0018-9294(02)02994-4.

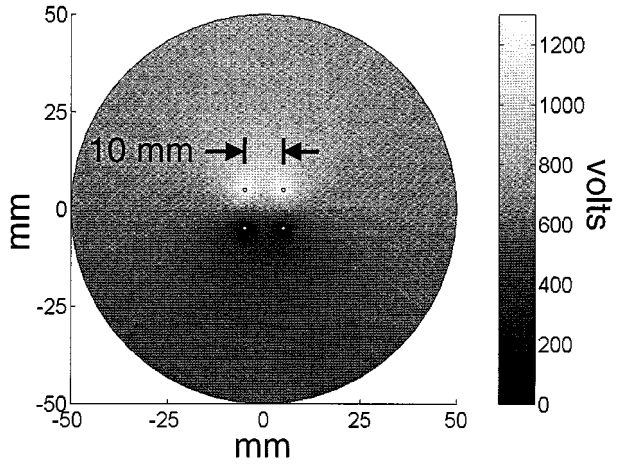

Fig. 1. Potential distribution for first configuration and general schematic (10 cm tissue, 1-mm electrodes, no flux exterior, and 1300 V/0 V).

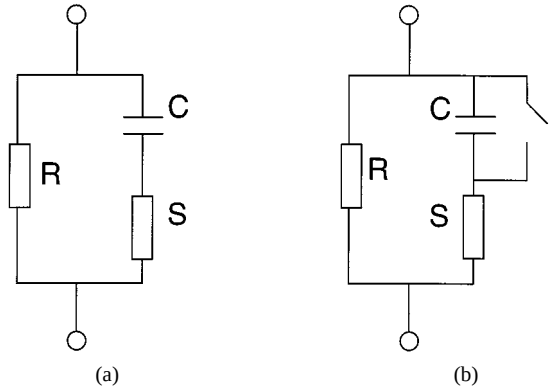

(a) (b)

Fig. 2. Electrical schematics for (a) The Cole–Cole model. (b) The model used in study. R represents the extracellular space, S the intracellular space, and C the membrane capacitance.

10 mm from one another, centered in the liver. The second configuration is similar to the first except that the spacing is only 6 mm, and the electrodes are positioned toward the upper left section of the liver. The final configuration uses only two electrodes, 10 mm apart, placed in the lower-right section of the tissue. All electrodes have a diameter of 1 mm.

In order to estimate the change in tissue electrical impedance during electroporation, we have used data from the experiments of Huang and Rubinsky [11]. In these experiments, performed with hepatocytes of rats, the change in electrical impedance of a single cell during reversible electroporation was measured. Measurements were taken by passing direct current through two electrodes separated by a dielectric membrane in a conductive solution. The membrane contained a 4-μm hole at its center that trapped individual cells to measure current through the cell. Results showed that the resistance of the cells to direct current (60-ms pulses) was essentially infinite prior to the electroporation, but during the electroporation pulse, this resistance dropped to approximately 29 kΩ.

To calculate the change in conductivity of the bulk tissue during electroporation, we created a model similar to the Cole–Cole model [10], [13]. The Cole–Cole model represents biological tissue using a resistor for the extracellular space in parallel with another resistor (the intracellular space) and capacitor (the cell membrane) in series. For our model, the membrane is modeled with an additional switch in parallel with the capacitor, which closes during electroporation but otherwise remains open (see Fig. 2). For the following calculations, we will only consider this switch and neglect the capacitor because its contribution to the real part of the solution is small at low frequencies [9], [13].

Hepatocytes are cubical cells with typical dimensions of 20–40 μm. For a solid block, resistance is equal to the thickness divided by the product of the cross-sectional area and conductivity. If we assume a cubic geometry for the cells and that the extracellular space is small compared with the intracellular space, this reduces to the reciprocal product between the cell length, 20 μm, and the tissue conductivity, 0.28 S/m at 20 kHz. (Tissue conductivity is taken from literature [13]). Therefore, the bulk tissue resistance prior to electroporation is 179 kΩ. Since we assume that the membrane does not allow current to flow prior to electroporation, this resistance, which remains constant, represents that of the extracellular space. During electroporation, this resistance is in parallel with the 29 kΩ resistance of the cell, which drops the entire resistance of the system (i.e., the tissue) to 25 kΩ. This resistance is converted back to conductivity using the same equation as before. Based on these assumptions, the conductivity of the tissue increases from 0.28 S/m to 2.0 S/m during electroporation.

The electroporation simulation is configured with the top electrodes at 1300 V and the bottom electrodes grounded, which are typical values for electrochemotherapy [8], [12]. The surface of the analyzed tissue is assumed to be electrically isolated with a zero flux boundary condition. We assume that the threshold gradient required to induce electroporation is 360 V/cm, which was reported by Mir [4] for rabbit liver cells. The finite-element model evaluates the potential distribution and voltage gradients, which are governed by the Poisson equation with a zero source term [3]

$$\nabla \cdot (\sigma \nabla \phi) = 0 \tag{1}$$

where σ is the electrical conductivity and ϕ is the electrical potential.

Previous methods for calculating the electroporated region shape of a given electrode configuration have relied on single-pass solvers [8], [12]. Our algorithm uses an iterative solution with multipass solvers to account for the change in electrical properties of the tissue during electroporation. Initially, the conductivity of the tissue is 0.28 S/m. At locations where the voltage gradient surpasses the threshold gradient of 360 V/cm, the conductivity increases to 2.0 S/m. On the next pass, the gradients are recalculated with the updated conductivity values. Again, conductivity is increased at locations above the threshold. This process is repeated until the solution converges. We assume that once a tissue changes conductivity, it does not revert back to the original value during the subsequent iterations regardless of whether the gradient falls below the threshold value. This assumption is based on studies that show that cells remain permeable for several minutes after the initial pulse [4]. From this calculation, a conductivity map is generated for the electroporated tissue.

The next step of this study uses the electroporation conductivity map as a simulated phantom for the EIT algorithm. Impedance imaging typically involves surrounding the region to be imaged with electrodes, injecting sinusoidal currents through combinations of electrodes pairs, and measuring the resulting voltages through the remaining electrodes. These measurements, along with current pair, current magnitude, and electrode geometry data are used by the reconstruction algorithm to produce an impedance image. For a general overview of EIT, see [9]. For our simulated phantom, 16 electrodes are equally spaced around the model periphery. A 1-mA current is injected through opposite electrode pairs (“projections”) while recording remaining opposite electrode pair voltages (known as an “opposite-opposite” data collection algorithm [14]), producing a vector of independent voltage measurements. This vector length defines the maximum number of independent variables (in our case, 104 impedance pixels) for a well-defined matrix inverse to exist. For each current projection, the resulting voltages are obtained by

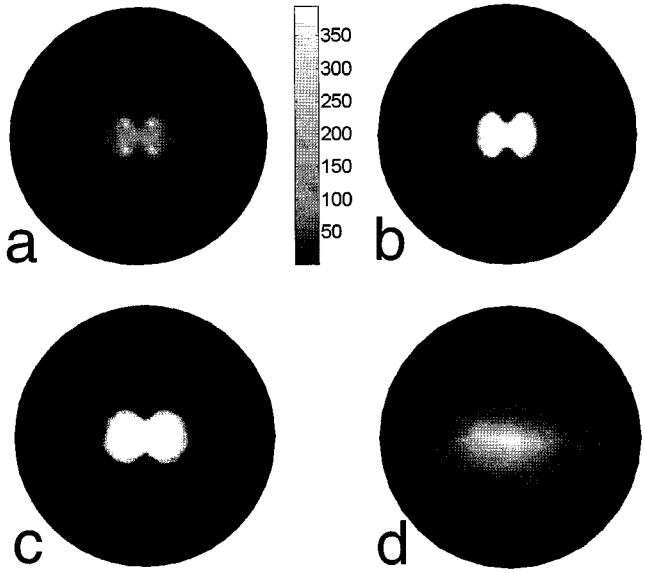

Fig. 3. (a) Gradient distribution [V/cm] pass one. (b) Conductivity map, pass one. (c) Converged conductivity map, pass 20. (d) Image.

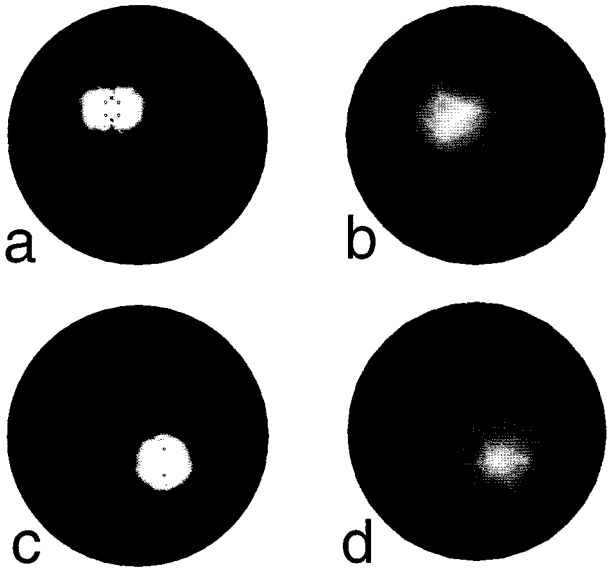

Fig. 4. (a) Conductivity map for second configuration (four electrodes in upper left region, 6-mm spacing). (b) Image of second configuration. (c) Conductivity map for third configuration (two electrodes in lower right region, 10-mm spacing). (d) Image of third configuration.

solving the Poisson equation in a finely meshed finite-element system using the converged electroporated impedance distribution ($\sim$ 6300 elements, $\sim$ 3200 nodes).

These independent voltages, current pair information, and electrode geometries from the simulated phantom are then used as inputs to our reconstruction algorithm. Of the numerous approaches to EIT reconstruction, we have chosen a modified Newton–Raphson (NR) method due to its excellent convergence properties [15]. This NR method attempts to iteratively minimize a cost function representing the overall voltage measurement differences between the simulated phantom and the reconstruction algorithm's internal model. The Jacobian needed for the NR method was calculated using a sensitivity matrix approach [16]. Marquardt regularization was used to overcome the ill conditioning of the Jacobian matrix [17]. Gaussian noise was added to each electrode measurement to determine the effects of noise image quality. No quantitative discernability studies were performed, but a decrease in image quality began as noise levels approached 1.0% of the maximum measured voltage amplitude. Because it is assumed that the EIT electrodes in this case study are internal and fixed in geometry, electrode placement uncertainty errors were not considered.

Our reconstruction algorithm's internal model consists of a finite-element mesh with an inner imaging region of 94 triangular elements, and a constrained outer ring of 120 elements at a constant, known background resistivity, resulting in an approximate resolution of 5 mm (square root of the average element area). It should be noted that finer resolutions could be obtained by increasing the number of electrodes but at a computational cost. The algorithm convergence criteria were typically met after approximately 20 iterations. All computations were done using MATLAB's partial differential equation toolbox (The MathWorks Inc., Natick, MA) and were performed on a Dell Precision 420 PC with an Intel 800-MHz processor.

III. Results

Imaging of a simulated electroporation process was performed for a liver using the three different electrode configurations mentioned above. Fig. 1 shows the potential distribution for the first configuration (four centered electrodes) and labels the relevant dimensions and boundary conditions. Fig. 3(a)–(d) shows the first configuration. Fig. 3(a) is the gradient distribution after the first iteration of our electroporation algorithm. Fig. 3(b) is a conductivity map generated using the information from Fig. 3(a). For elements above the threshold gradient of 360 V/cm, the conductivity is increased to our value for permeated tissue, 2.0 S/m. The results from Fig. 3(b) are used to recalculate the gradient until the solution converges. Fig. 3(c) is the conductivity map for the converged solution. The difference between Fig. 3(b) and (c) demonstrates the improvement of iterative over single-pass algorithms in their ability to produce a more complete and accurate permeability distribution. This distribution is then passed to the EIT imaging module, and Fig. 3(d) shows the generated image using our reconstruction algorithm.

Fig. 4(a)–(d) shows other examples to show the robustness of the technique. Fig. 4(a) is a conductivity map for a four-electrode configuration with 6-mm spacing located in the upper left section of the tissue. Fig. 4(b) is the generated image. Fig. 4(c) is a conductivity map of the electroporated region for a two-electrode configuration, in which the two are 10 mm apart and located in the bottom-right of the tissue. Fig. 4(d) is the corresponding image. Notice that in both cases, the EIT algorithm was able to reconstruct images representing both the size and placement of the electroporated region.

Currently, electroporation and engineered retroviruses are the most common methods to introduce macromolecules into cells *in vivo*. To the best of our knowledge, however, there is no procedure to actively monitor or control these techniques. This is one of the largest obstacles inhibiting the effective treatment of patients. The use of engineered retroviruses has actually led to significant complications and the loss of life because of the lack of ability to localize and control the genetic treatment. This theoretical study demonstrates that real-time monitoring of molecular medicine *in vivo* can be achieved through the synthesis of two fairly well understood techniques, electroporation and EIT.

It should be noted that these results, however promising, are still theoretical and much more work remains before this method becomes a clinical technique. First of all, real world experiments must be performed. There are also several improvements that could be implemented in future models. For example, we have modeled the liver as a homogeneous tissue, ignoring possible conductivity perturbations from larger blood vessels. Other real world complexities,

including the inherently three-dimensional nature of EIT and more realistic electrode models, will be the subject of future investigations and are not considered in this preliminary study. Another potential improvement would incorporate the interior electrodes used for electroporation to help generate the image.

IV. Summary

In this study, we have examined the hypothesis that the decrease in electrical impedance associated with electroporation should be detectable using a bioimpedance technique. We tested this hypothesis by applying an EIT algorithm to three different electroporation simulations of the liver. In all three scenarios the electroporated regions were clearly distinguishable. It should be noted that this is a preliminary demonstration, and much work remains to bring this technique to clinical practice. Nevertheless, the results of the study demonstrate the potential of EIT for monitoring *in vivo* electroporation.

References

[1] S. Somiari *et al.*, "Theory and *in vivo* application of electroporative gene delivery," *Mol. Ther.*, vol. 2, pp. 178–187, Sept. 2000.

[2] J. C. Weaver, "Electroporation of cells and tissues," *IEEE Trans. Plasma Sci.*, vol. 28, pp. 24–33, Feb. 2000.

[3] R. Davalos, B. Rubinsky, and Y. Huang, "Electroporation: bio-electrochemical mass transfer at the nano scale," *Microscale Thermophysical Eng.*, vol. 4, pp. 147–159, 2000.

[4] L. M. Mir, "Therapeutic perspectives of *in vivo* cell electropermeabilization," *Bioelectrochem.*, vol. 53, pp. 1–10, 2000.

[5] M. Okino and H. Mohri, "Effects of a high-voltage electrical impulse and anticancer drugs on *in vivo* growing tumors," *Jpn. J. Cancer Res.*, vol. 78, pp. 1319–1321, Dec. 1987.

[6] L. M. Mir, S. Orlowski, J. Belehradek, and C. Paoletti, "Electrochemotherapy: potentiation of antitumour effect of bleomycin by local electric pulses," *Eur. J. Cancer*, vol. 27, pp. 68–72, May 1991.

[7] M. J. Jaroszeski, R. Heller, and R. Gilbert, *Electrochemotherapy, Electrogenetherapy, and Transdermal Drug Delivery: Electrically Mediated Delivery of Molecules to Cells*. Totowa, NJ: Humana, 2000.

[8] D. Miklavcic, D. Semrov, H. Mekid, and L. M. Mir, "A validated model of *in vivo* electric field distribution in tissues for electrochemotherapy and for DNA electrotransfer for gene therapy," *Biochim. Biophys. Acta.*, vol. 1523, pp. 73–83, January 2000.

[9] J. G. Webster, *Electrical Impedance Tomography*. New York: Adam Higler, 1990, pp. 75–86.

[10] J. D. Bronzino, *The Biomedical Engineering Handbook*, 2nd ed. Boca Raton, FL: CRC, 2000, vol. 68, pp. 1–9.

[11] Y. Huang and B. Rubinsky, "Micro-electroporation: improving the efficiency and understanding of electrical permeabilization of cells," *Biomed. Microdevices*, vol. 2, pp. 145–150, 1999.

[12] D. Miklavcic *et al.*, "The importance of electric field distribution for effective *in vivo* electroporation of tissues," *Biophys. J.*, vol. 74, pp. 2152–2158, May 1998.

[13] K. Boone, D. Barber, and B. Brown, "Imaging with electricity: Report of the European concerted action on impedance tomography," *J. Med. Eng. Technol.*, vol. 21, pp. 201–232, Nov. 1997.

[14] B. Rigaud and J. P. Morucci, "Bioelectrical impedance techniques in medicine: Part III: Impedance imaging: First section: general concepts and hardware," *Crit. Rev. Biomed. Eng.*, vol. 24, pp. 467–597, Aug. 1996.

[15] T. J. Yorkey and J. G. Webster, "A comparison of impedance tomographic reconstruction algorithms," *Clin. Phys. Physiol. Meas.*, vol. 8, pp. 55–62, June 1987.

[16] N. G. Gencer, Y. Z. Ider, and S. J. Williamson, "Electrical impedance tomography: Induced-current imaging achieved with a multiple coil system," *IEEE Trans. Biomed. Eng.*, vol. 43, pp. 139–149, Aug. 1996.

[17] D. W. Marquardt, "An algorithm for least-squares estimation of nonlinear parameters," *J. Appl. Math.*, vol. 11, pp. 431–441, 1963.